Archivos de Bronconeumología xxx (xxxx) xxx–xxx

Sociedad Española de Neumología y Cirugía Torácica SEPAR

ARCHIVOS DE
Bronconeumología

www.archbronconeumol.org

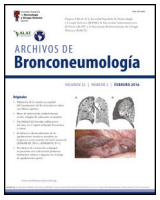

Original Article

Revisiting REVEAL-ECHO: A Focus on Pulmonary Veno-Occlusive Disease

Eva Gutiérrez-Ortiz[a,b,c,d], Carmen Jiménez López-Guarch[a,b,c,d,e,f], Alejandro Cruz-Utrilla[a,b,c,e,*], Julia Playan-Escribano[d,g], Celia Denche Sanz[a], Sergio Alonso Charterina[d,h], Maite Velázquez[a,b,c,e,i], Berenice Brown[a], Irene Martín De Miguel[a,b,c], Carlos Andrés Quezada Loaiza[a,b,c,j], Fernando Arribas Ynsaurriaga[a,b,c,d,e], Pilar Escribano-Subias[a,b,c,d,e]

[a] *Pulmonary Hypertension Unit, Department of Cardiology, Hospital Universitario 12 de Octubre, Madrid, Spain*
[b] *ERN-LUNG (European Reference Network on Rare Respiratory Diseases), Frankfurt am Main, Germany*
[c] *Instituto de Investigación Hospital 12 de Octubre (i+12), Madrid, Spain*
[d] *Facultad de Medicina, Universidad Complutense de Madrid, Madrid, Spain*
[e] *Centro de Investigación Biomédica en Red de Enfermedades Cardiovasculares (CIBERCV), Madrid, Spain*
[f] *Cardiac Imaging Unit, Department of Cardiology, Hospital Universitario 12 de Octubre, Madrid, Spain*
[g] *Department of Cardiology, Hospital General Universitario Gregorio Marañón, Instituto de Investigación Sanitaria del Hospital Gregorio Marañón, Hospital Universitario del Sureste, Arganda del Rey, Spain*
[h] *Cardiothoracic Radiology Unit, Department of Radiology, Hospital Universitario 12 de Octubre, Madrid, Spain*
[i] *Interventional Cardiology Unit, Department of Cardiology, Hospital Universitario 12 de Octubre, Madrid, Spain*
[j] *Lung Transplantation Unit, Department of Pneumology, Hospital Universitario 12 de Octubre, Madrid, Spain*

ARTICLE INFO

Article history:
Received 29 January 2026
Accepted 2 May 2026
Available online xxx

Keywords:
Pulmonary veno-occlusive disease
Pulmonary arterial hypertension
REVEAL-ECHO
Risk stratification

ABSTRACT

Background: Pulmonary veno-occlusive disease (PVOD) is a severe subtype of pulmonary arterial hypertension (PAH) with especially poor prognosis. Existing risk scores, such as REVEAL Lite 2.0 and REVEAL-ECHO, were not developed in cohorts with high PVOD prevalence. This study aimed to characterize echocardiographic remodeling in PVOD; to evaluate predictive performance of REVEAL-ECHO for mortality and lung transplantation (LT); and to develop a PVOD-adapted version of REVEAL-ECHO score.
Methods: A retrospective cohort of 282 PAH patients was analyzed, including 50 PVOD patients. PVOD diagnosis was based on histological confirmation, genetic testing, or compatible clinical and radiological features. Risk was stratified using REVEAL Lite 2.0, the original REVEAL-ECHO model, and a PVOD-modified REVEAL-ECHO model. A combined 4-strata score integrating REVEAL Lite 2.0 with the modified model was also evaluated.
Results: PVOD patients exhibited worse right ventricular remodeling despite similar hemodynamics. REVEAL Lite 2.0 outperformed the original REVEAL-ECHO model, whereas incorporation of PVOD etiology significantly improved the echocardiography-based model. The 4-strata PVOD model showed the best overall prognostic performance, with the highest discrimination and improved reclassification of adverse outcomes across all evaluated endpoints. Concordant low-risk classification by both clinical and echocardiographic models identified a subgroup with a high negative predictive value.
Conclusions: Incorporating PVOD etiology into REVEAL-ECHO score improves its predictive accuracy and refines risk stratification in cohorts with high PVOD prevalence. Integrating etiology with clinical and echocardiographic assessment enhances risk discrimination and may support more individualized decision-making regarding transplant listing timing, including identification of a low-risk subgroup in whom listing could be deferred.

© 2026 SEPAR. Published by Elsevier España, S.L.U. All rights are reserved, including those for text and data mining, AI training, and similar technologies.

Introduction

Pulmonary arterial hypertension (PAH) is a progressive, life-threatening condition driven by pulmonary vascular remodeling

* Corresponding author.
E-mail address: alejandro.cruz@salud.madrid.org (A. Cruz-Utrilla).

https://doi.org/10.1016/j.arbres.2026.05.002
0300-2896/© 2026 SEPAR. Published by Elsevier España, S.L.U. All rights are reserved, including those for text and data mining, AI training, and similar technologies.

Please cite this article as: E. Gutiérrez-Ortiz, C. Jiménez López-Guarch, A. Cruz-Utrilla et al., Revisiting REVEAL-ECHO: A Focus on Pulmonary Veno-Occlusive Disease, Archivos de Bronconeumología, https://doi.org/10.1016/j.arbres.2026.05.002

that culminates in right ventricular (RV) failure and premature death. Contemporary management, based on risk stratification, aims to achieve and maintain a low-risk profile; however, many patients classified outside the high-risk category still experience adverse outcomes, which highlights the limitations of current algorithms [1,2].

Non-invasive imaging, particularly echocardiography, offers clinical insights into RV structure and function and may improve prognostic assessment [3–6]. Building on this concept, REVEAL-ECHO (R-Echo) integrates echocardiographic parameters into the REVEAL framework to enhance risk stratification beyond clinical and hemodynamic data [3].

Within the spectrum of PAH, pulmonary veno-occlusive disease (PVOD) represents one of the most aggressive phenotypes [1]. It is characterized by severe hypoxemia with markedly reduced diffusing capacity of the lung for carbon monoxide (DLCO) secondary to venular and capillary remodeling, and by poor tolerance to vasodilator therapy due to the risk of pulmonary edema. In this clinical context, bilateral lung transplantation (LT) remains the only treatment alternative [7].

In Spain, PVOD has been reported as relatively more frequent, partly due to *EIF2AK4*-related familial clusters among Iberian Romani patients [8–10]. Data from the Spanish Registry of Pulmonary Hypertension (REHAP) reported a prevalence of 6.6% [11], which is higher than figures from REVEAL or French registries [12,13]. At the same time, Spain offers a unique setting to address this condition given its high organ donation and LT rates [14].

Although existing PAH risk models perform adequately in general populations, PVOD patients show higher mortality, even within low risk strata [15,16]. This excess mortality suggests that factors beyond those included in current risk assessment tools may contribute to prognosis in PVOD-rich cohorts, including treatment response, susceptibility to pulmonary edema, and progressive respiratory insufficiency. Despite the high incidence of adverse events, there is heterogeneity in disease course and survival [15–17]. This variability highlights the need for refined risk stratification tools capable of identifying patients at imminent risk of deterioration and optimizing timely listing for LT.

To date, no study has specifically assessed RV remodeling in PVOD or tested imaging-based risk models in cohorts enriched for PVOD. Because most risk scores analyzed mortality as the primary endpoint, incorporating LT as a competing outcome is relevant in this population. Therefore, the present study aims to: (1) describe RV remodeling in PVOD patients; (2) assess the prognostic performance of R-Echo for the combined endpoint of death or LT in a cohort representative of a population with frequent PVOD, and (3) develop a modified version of the model, adapted to this population, to improve risk stratification.

Methods

Study population

We performed a retrospective cohort study at a tertiary referral center participating in the Spanish nationwide REHAP registry. All consecutive patients enrolled between January 2017 and January 2024 were screened. The study was approved by the institutional ethics committee (CEIM 16/102), and all participants provided written informed consent.

Adults (≥18 years) with pre-capillary pulmonary hypertension (PH) confirmed by right heart catheterization were eligible, in accordance with the 2015 ESC/ERS criteria [18]. We excluded patients with chronic thromboembolic PH, Eisenmenger syndrome, overlapping etiologies, and missing echocardiography or risk-stratification data.

PVOD was diagnosed by histological or genetic confirmation, or by multidisciplinary consensus based on clinical and radiological criteria. Histological diagnosis required typical venular and capillary remodeling; genetic diagnosis was established by a homozygous or compound heterozygous pathogenic variant in *EIF2AK4*. In the remaining cases, diagnosis was based on a severely reduced DLCO and at least two of three characteristic radiological findings (septal lines, ground-glass opacities, mediastinal lymphadenopathy) [7,19].

Risk stratification

Patients were classified according to clinical, echocardiography-based and combined clinical–echocardiographic scores. As the clinical model, we used the REVEAL Lite 2.0 risk score (R-Lite) [20]. As the echocardiographic model, we applied the original R-Echo score, which incorporates RV enlargement, RV systolic function, tricuspid regurgitation severity, and pericardial effusion, and accounts for PAH etiology (PVOD was not included in the original derivation cohort) [3].

To adapt the echocardiographic model to a cohort with a high prevalence of PVOD, we developed a modified version that incorporated PVOD etiology as an additional variable. Using the same weighting strategy as in the original R-Echo model, in which variables with hazard ratios ≥3 were assigned 3 points, PVOD was assigned 3 points because it was associated with mortality in Cox regression analysis (HR 5.57, 95% CI 2.28–13.58; $p < 0.001$). This modified score was termed R-Echo-PVOD. For both echocardiography-based models (R-Echo and R-Echo-PVOD), data were extracted from the first transthoracic echocardiogram performed at our center; therefore, the cohort included both incident and prevalent patients.

Finally, patients were reclassified using combined clinical–echocardiographic models that integrated R-Lite with R-Echo-PVOD. In this framework, patients at low risk by both R-Lite and R-Echo-PVOD were classified as low-risk; those with low-risk R-Lite but intermediate- or high-risk R-Echo-PVOD as intermediate-low-risk category; all patients at intermediate risk by R-Lite as intermediate-high-risk category; and all patients at high risk by R-Lite remained high-risk. This yielded a 4-strata combined model, termed 4-strata R-Echo-PVOD. Fig. 1S shows patient risk stratification workflow.

Statistical analysis

Continuous variables are expressed as median (interquartile range) and categorical as *n* (%). The primary endpoint was clinical worsening (all-cause mortality or LT). Follow-up was calculated from inclusion to the occurrence of the endpoint or last available evaluation and was truncated at 5 years for all analyses. Model performance was primarily assessed at 5 years; for greater comparability with the R-Lite score, analyses were also performed at 1 year.

Survival was analyzed using Kaplan–Meier estimates and log-rank tests. Associations between risk categories and LT-free survival were assessed by multivariable Cox regression. The proportional hazards assumptions were verified with Schoenfeld residuals (all $p > 0.05$). Given the presence of competing events, competing-risk analyses were performed using Fine–Gray subdistribution hazard models, considering LT as a competing event for all-cause mortality.

Model performance was evaluated using Harrell's C-index, time-dependent area under the curve (AUC) analysis and the Akaike Information Criterion (AIC). These analyses were conducted separately for each risk stratification approach. To further characterize the prognostic performance of the risk strata, negative predictive

values for the low-risk category and positive predictive values for the high-risk category were assessed across models. Reclassification between models was assessed using the net reclassification improvement (NRI). AUCs were compared using DeLong's test, and C-indices by pairwise comparison.

Internal validation of discrimination at 1 and 5 years was performed for the modified models using 1000 bootstrap resampling, in line with TRIPOD guidelines recommendations (Transparent Reporting of a multivariable prediction model for Individual Prognosis Or Diagnosis) [21]. In each resample, the HR for PVOD was recalculated, and the score was assigned accordingly, using the same threshold-based weighting strategy as the original R-Echo model. This approach assessed the stability of the PVOD weighting strategy in the model derived from the full cohort. Optimism was estimated as the difference between model performance in the bootstrap sample (apparent) and in the original sample (test). Results were summarized as mean optimism with 95% confidence intervals based on the 2.5th and 97.5th percentiles of the bootstrap distribution. Bootstrap validation was applied only to R-Echo-PVOD and 4-strata R-Echo-PVOD, which were developed in our cohort.

All statistical analyses and graphs were conducted with Stata 16 (Stata Corp).

Results

Clinical characteristics and RV remodeling

A total of 311 patients were initially identified. Twelve patients were excluded due to Eisenmenger syndrome, 2 due to incomplete data for risk score calculation, 2 due to missing follow-up data, and 10 due to combined etiology and 3 who were reclassified as Group 5 after comprehensive etiological evaluation. The final cohort had 282 patients, including 50 with PVOD.

Characteristics at baseline are shown in Table 1. Median age was 51.9 years and 67.7% were female. Idiopathic PAH was the most frequent etiology, followed by connective tissue disease-associated PAH and PVOD. Among patients with PVOD, 6 had a genetically confirmed diagnosis based on *EIF2AK4* mutations, 14 were histologically confirmed following LT and 30 were diagnosed based on clinical and radiological features. Of the 14 patients with histological confirmation after LT, 4 already had prior genetic confirmation, 1 had been diagnosed with lung biopsy, and 9 fulfilled non-invasive diagnostic criteria.

PVOD patients showed more advanced RV remodeling and dysfunction despite similar hemodynamics. Treatment patterns were similar across PVOD diagnostic subgroups, except that dual oral therapy was more frequent in histopathology-confirmed than in genetically confirmed PVOD ($p = 0.020$). Tobacco exposure and cardiovascular comorbidity burden did not differ by diagnostic method ($p = 0.184$ and $p = 0.533$).

Seventy-four patients (26.2%) presented clinical worsening (50 deaths and 24 LT). The overall 1-, 3-, and 5-year transplant-free survival rates in this cohort were 87.3% (82.7–90.7), 74.2% (68.1–79.3), and 67.6% (60.6–73.7), respectively.

PVOD was associated with significantly higher mortality and LT rates than non-PVOD. In time-to-event analysis, PVOD was associated with a markedly increased hazard of LT (HR 9.92, 95% CI 4.26–23.09; $p < 0.001$). Notably, 50% of LT in the PVOD group were performed under urgent conditions. Mean time to LT listing was 12.9 ± 15.6 months in PVOD patients and 16.1 ± 24.4 months in non-PVOD patients, with no statistically significant differences between groups ($p = 0.756$).

Risk stratification and outcome analysis

After incorporating PVOD as an additional weighted variable, the R-Echo-PVOD model reclassified 12.8% of patients to a higher risk category compared with the original R-Echo model, mainly from the low- and intermediate-risk groups (Table 1S). The Sankey plots illustrate how patients were redistributed across risk strata when comparing R-Lite with R-Echo-PVOD, together with the corresponding event rates observed for each endpoint (Fig. 1).

A stepwise risk gradient for the composite endpoint was observed with both R-Lite and R-Echo-PVOD, whereas the original R-Echo model showed only modest separation (Table 2). LT-free survival discrimination was significantly stronger for R-Lite and R-Echo-PVOD ($\chi^2 = 34.35$ and 20.07; both $p < 0.001$) than for R-Echo ($\chi^2 = 5.79$; $p = 0.055$). Competing-risk analyses yielded consistent results (Table 2S).

Comparisons across risk strata for all prognostic models are shown in Table 3S. Overall, R-Lite and the PVOD-adjusted R-Echo models both showed good separation between risk categories for the composite endpoint. For the individual endpoints, R-Lite showed clearer discrimination for mortality, whereas the R-Echo-PVOD model showed better separation for LT. Fig. 2 displays the corresponding Kaplan–Meier curves, which showed consistent results.

Patient redistribution according to the 4-strata R-Echo-PVOD model is shown in Table 3. This configuration showed a progressive increase in event rates across risk categories. Discrimination across strata was robust, with significant separation in most pairwise comparisons and borderline significance in the remaining adjacent-strata comparisons.

Comparative model performance

Performance metrics for all risk stratification models are summarized in Table 4. R-Lite showed better discrimination than the original R-Echo (C-index $p < 0.001$; AUC $p = 0.002$). Adding the PVOD-specific adjustment strengthened the echocardiographic model: R-Echo-PVOD improved on R-Echo (both C-index and AUC $p = 0.001$). The 4-strata R-Echo-PVOD showed the best overall performance and was superior to R-Lite (C-index $p = 0.042$; AUC $p = 0.047$). Across models, discriminative performance was consistently higher at 1 year than at 5 years.

Internal validation results are shown in Table S4. Optimism was low across all evaluated metrics (<0.01), with 95% confidence intervals including 0. Therefore, estimated performance in comparable new samples was similar to the apparent performance.

NRI results are shown in Table 5S. R-Echo-PVOD improved event reclassification compared with both the original R-Echo (+24.3%) and R-Lite (+8.1%), at some loss of specificity among non-events. This effect was more pronounced in transplant-focused analyses, where 20% of transplant recipients were correctly reclassified into higher-risk strata, with positive overall NRI values. Similarly, the 4-strata R-Echo-PVOD model also improved reclassification performance, showing positive NRI values across all examined outcomes.

Among transplanted patients, the mean time from baseline evaluation to inclusion on the waiting list decreased across increasing risk categories in all models. In the R-Lite model, mean time to listing was 36.0, 14.5, and 5.9 months for low-, intermediate-, and high-risk patients, respectively ($\rho = -0.54$, $p = 0.006$). In the R-Echo model, the corresponding values were 24.3, 12.6, and 7.5 months, with a non-significant association between risk category and time to listing ($p = 0.218$). In the R-Echo-PVOD model, the low-risk group showed the longest time to listing (46.2 months), whereas intermediate- and high-risk patients showed mean times of 22.2 and 5.9 months, respectively ($\rho = -0.55$, $p = 0.005$).

Table 1
Baseline characteristics global cohort.

	Global cohort N = 282	Non-PVOD N = 232	PVOD N = 50	p value
Demographics				
Female	191 (67.7)	164 (70.7)	27 (54.0)	0.022
BMI, kg/m²	25.6 (22.0–29.9)	25.7 (22.0–30.4)	24.7 (21.4–28.3)	0.247
Age, years	51.9 (39.6–63.4)	51.6 (39.1–63.3)	53.9 (41.2–65.0)	0.603
Prevalent patients	146 (51.8)	108 (46.6)	14 (28.0)	0.016
PAH etiology				
Idiopathic	84 (29.8)	84 (36.2)	0 (0.0)	N/A
Connective tissue disease	57 (20.2)	57 (24.6)	0 (0.0)	
PVOD	50 (17.7)	0 (0.0)	50 (100.0)	
EIF2AK4 biallelic mutation	6 (2.1)	0 (0.0)	6 (12.0)	
Histological confirmation	10 (3.5)	0 (0.0)	10 (20.0)	
Radiological and clinical criteria	30 (10.6)	0 (0.0)	30 (60.0)	
Histological and genetical confirmation	4 (1.4)	0 (0.0)	4 (8.0)	
Corrected/incidental CHD	24 (8.5)	24 (10.3)	0 (0.0)	
Heritable	22 (7.8)	22 (9.5)	0 (0.0)	
PoPH	22 (7.8)	22 (9.5)	0 (0.0)	
Drugs/Toxins	7 (2.5)	7 (3.0)	0 (0.0)	
HIV	7 (2.5)	7 (3.0)	0 (0.0)	
Long-term responders to CCB	9 (3.2)	9 (3.9)	0 (0.0)	
Hemodynamics				
RAP, mmHg	8 (5–11)	8 (5–12)	7 (5–10)	0.215
PAPm, mmHg	48 (39–57)	49 (40–58)	47 (37–55)	0.200
PAWP, mmHg	11 (8–13)	11 (8–13)	11 (6–12)	0.375
CO, L/min	4.5 (3.5–5.5)	4.5 (3.5–5.6)	4.3 (3.5–5.1)	0.464
CI, L/min/m²	2.4 (2.0–3.0)	2.5 (2.0–3.0)	2.3 (2.0–2.7)	0.235
PVR, WU	8.4 (5.9–12.1)	8.5 (5.9–12.2)	7.4 (5.8–11.9)	0.502
Labs				
NTproBNP, pg/mL	461 (145–1527)	420 (138–1527)	819 (219–1543)	0.236
Glomerular filtrate rate, ml/min, 1.73 m²	90 (67–90)	90 (70–90)	90 (60–90)	0.467
Clinical data				
Systolic arterial pressure (mmHg)	115 (102–127)	116 (104–130)	110 (91–122)	0.003
Heart rate (bpm)	83 (73–93)	82 (73–94)	86 (75–93)	0.213
6MWT distance (m)	375 (300–480)	394 (322–489)	282 (238–373)	<0.001
WHO Functional Class				
I–II	143 (50.7)	125 (53.9)	18 (36.0)	0.020
III	117 (41.6)	93 (40.1)	24 (48.0)	0.303
IV	21 (7.5)	13 (5.6)	8 (16.0)	0.011
Echocardiography				
RV basal diameter (mm)	44 (40–50)	44 (40–51)	45 (41–48)	0.988
RV basal diameter index (mm/m²)	25.6 (22.0–28.7)	25.5 (21.6–28.8)	25.6 (23.0–28.5)	0.993
RV/LV basal diameter ratio	1.2 (1.0–1.4)	1.2 (1–1.4)	1.3 (1.2–1.4)	0.038
Diastolic eccentricity index	1.3 (1.1–1.6)	1.2 (1.0–1.4)	1.4 (1.1–1.6)	0.067
TAPSE (mm)	18 (15–22)	19 (16–22)	17 (15–19)	0.006
S′ wave (cm/s)	11 (9–13)	11 (9–13)	10 (9–12)	0.032
Right atrium area (cm²)	20 (16–25)	20 (16–26)	19 (16–24)	0.410
Estimated PASP (mmHg)	72 (54–90)	71 (53–90)	80 (67–92)	0.068
TAPSE/PASP (mm/mmHg)	0.24 (0.18–0.36)	0.25 (0.18–0.39)	0.22 (0.16–0.27)	0.034
Tricuspid regurgitation				
None or mild	171 (60.6)	140 (60.3)	31 (62.0)	0.828
Moderate	85 (30.1)	69 (29.7)	16 (32.0)	0.752
Severe	26 (9.2)	23 (9.9)	3 (6.0)	0.386
Pericardial effusion				
None	235 (83.3)	195 (84.1)	40 (80.0)	0.486
Mild	37 (13.1)	29 (12.5)	8 (16.0)	0.506
Moderate	6 (2.1)	5 (2.2)	1 (2.0)	0.945
Severe	4 (1.4)	3 (1.3)	1 (2.0)	0.701
Treatment				
None	108 (38.3)	86 (37.1)	22 (44.0)	0.360
Oral monotherapy	32 (11.4)	28 (12.1)	4 (8.0)	0.411
Systemic prostanoid monotherapy	5 (1.8)	2 (0.9)	3 (6.0)	0.013
Double: PDE5i/Riociguat + ERA	78 (27.7)	67 (28.9)	11 (22.0)	0.324
Double with systemic prostanoid	6 (2.1)	4 (1.7)	2 (4.0)	0.312
PDE5i/Riociguat + ERA + Selexipag	19 (6.7)	15 (6.5)	4 (8.0)	0.695
PDE5i + ERA + systemic prostanoid	34 (12.1)	30 (12.9)	4 (8.0)	0.331
Events				
Death	50 (17.7)	33 (14.2)	17 (34.0)	0.001
Lung transplantation	24 (8.5)	10 (4.3)	14 (28.0)	<0.001
Urgent lung transplantation	9 (3.2)	2 (0.9)	7 (14.0)	<0.001

BMI: body mass index; CCB: calcium channel blockers; CHD: congenital heart disease, CI: cardiac index; CO: cardiac output; HIV: human immunodeficiency virus; ERA: endothelin receptor antagonist; PDE5i: phosphodiesterase type 5 inhibitor; PAH: pulmonary arterial hypertension; PAPm: mean pulmonary artery pressure; PASP: pulmonary artery systolic pressure; PAWP: pulmonary artery wedge pressure; PoPH: portopulmonary hypertension; PVOD: pulmonary veno-occlusive disease; PVR: pulmonary vascular resistance; RAP: right atrial pressure; RV: right ventricle; S′ wave: systolic velocity of the tricuspid annulus by tissue Doppler; TAPSE: tricuspid annular plane systolic excursion.

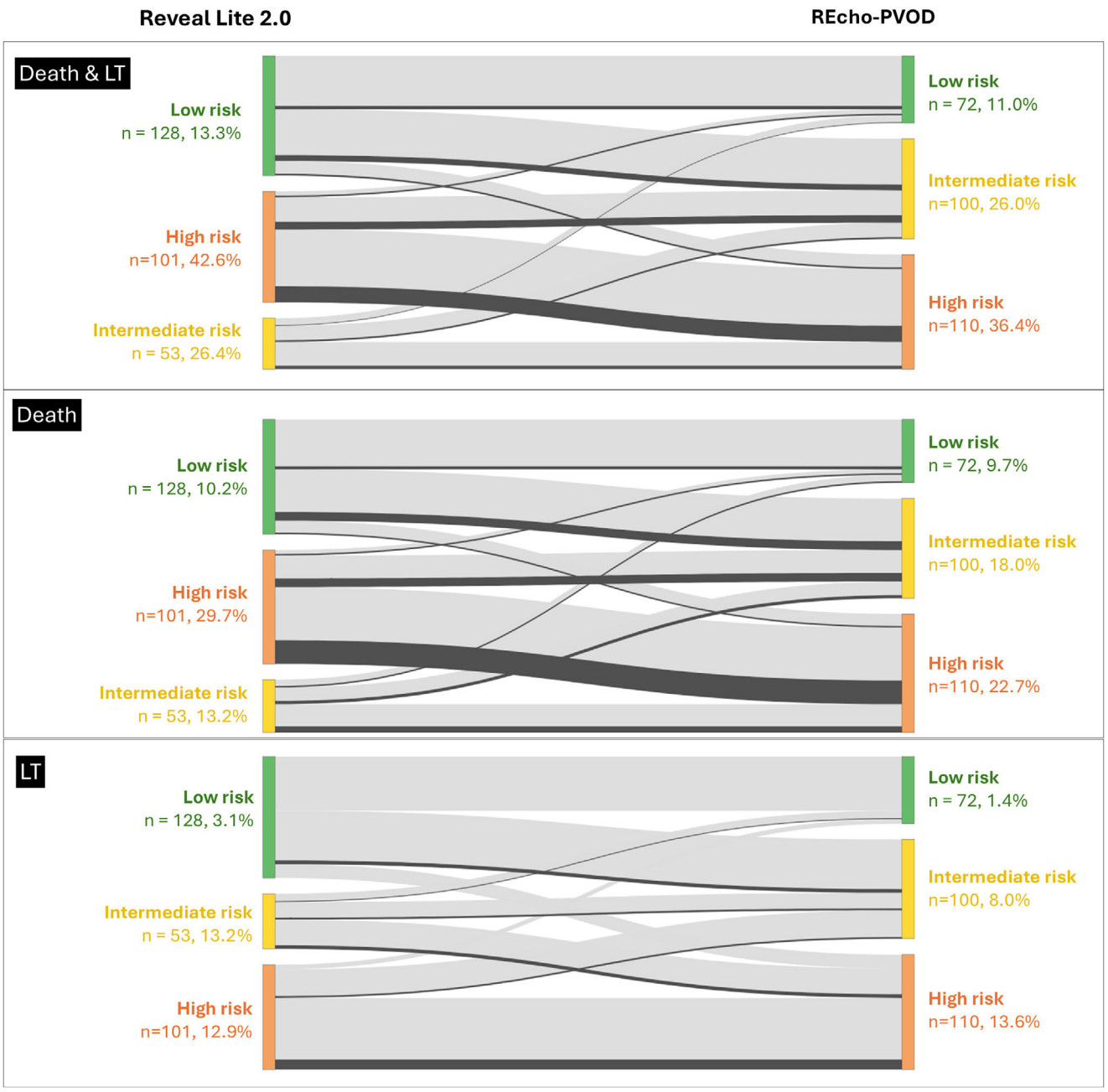

Fig. 1. Sankey diagrams illustrating patient reclassification between REVEAL Lite 2.0 and the R-Echo-PVOD model across three outcomes: combined endpoint (death or lung transplantation), death, and lung transplantation. Flows represent transitions between low-, intermediate-, and high-risk categories and percentages correspond to event rates within each category. LT: lung transplantation; REcho-PVOD: PVOD-adjusted REVEAL-Echo score; R-Lite: Reveal Lite 2.0.

Concordant low-risk classification in both models, which defines the low-risk category in the 4-strata model, showed the highest negative predictive value for adverse outcomes, with a negative predictive value of 93.2% for death and for the composite endpoint of death or LT, and 100% for LT alone (Table 6S).

Discussion

In this study, we provide a comprehensive evaluation of risk stratification tools in a large cohort of patients with PAH, with a particular focus on PVOD. Our main findings can be summarized as follows: (1) PVOD patients exhibited more adverse RV remodeling despite similar hemodynamic profiles compared with non-PVOD; (2) R-Lite demonstrated superior prognostic accuracy compared with the original R-Echo, with significantly better discrimination and calibration; (3) the inclusion of PVOD, a well-established marker of poor prognosis, as a weighted variable significantly improved the performance of the R-Echo score in a population with a high prevalence of this condition; and (4) R-Echo-PVOD and its 4-strata version improved reclassification of patients with events compared with the non-PVOD-adjusted models. Moreover, combining clinical and echocardiographic risk models yielded a high negative predictive value for adverse outcomes, especially in LT.

To our knowledge, this is the first study to characterize echocardiographic remodeling in PVOD and to evaluate imaging-based risk stratification models for predicting the relevant composite endpoint of death or LT in a cohort with a high prevalence of this condition.

Our findings reveal that PVOD patients had worse RV remodeling—greater dilation and reduced systolic

Table 2
Cox regression hazard ratios and event rates for death or lung transplantation according to risk categories defined by REVEAL Lite 2.0, REVEAL-ECHO, PVOD-modified REVEAL ECHO and 4-strata PVOD REVEAL ECHO.

	HR CI 95%	*p*-Value	Death	LT	Death or LT
R-Lite					
Low risk	–	–	13/128 (10.2)	4/128 (3.1)	17/128 (13.3)
Intermediate risk	2.65 (1.30–5.40)	0.007	7/53 (13.2)	7/53 (13.2)	14/53 (26.4)
High risk	4.88 (2.77–8.60)	<0.001	30/101 (29.7)	13/101 (12.9)	43/101 (42.6)
R-Echo					
Low risk	–		12/90 (13.3)	7/90 (7.8)	19/90 (21.1)
Intermediate risk	1.18 (0.64–2.15)	0.596	17/98 (17.3)	7/98 (7.1)	24/98 (24.5)
High risk	1.94 (1.09–3.45)	0.025	21/94 (22.3)	10/94 (10.6)	31/94 (33.0)
R-Echo-PVOD					
Low risk	–	–	7/72 (9.7)	1/72 (1.4)	8/72 (11.0)
Intermediate risk	2.45 (1.11–5.42)	0.027	18/100 (18.0)	8/100 (8.0)	26/100 (26.0)
High risk	4.51 (2.10–9.67)	<0.001	25/110 (22.7)	15/110 (13.6)	40/110 (36.4)
4-strata-R-Echo-PVOD					
Low risk	–	–	4/59 (6.8)	0/59 (0.0)	4/59 (6.8)
Inter-low risk	2.79 (0.91–8.55)	0.073	9/69 (13.0)	4/69 (5.8)	13/69 (18.8)
Inter-high risk	5.21 (1.71–15.85)	0.004	7/53 (13.2)	7/53 (13.2)	14/53 (26.4)
High risk	9.58 (3.43–26.77)	<0.001	30/101 (29.7)	13/101 (12.9)	43/101 (42.6)

CI: confidence interval; HR: hazard ratio; inter-low: intermediate-low risk; inter-high: intermediate-high risk; LT: lung transplantation.

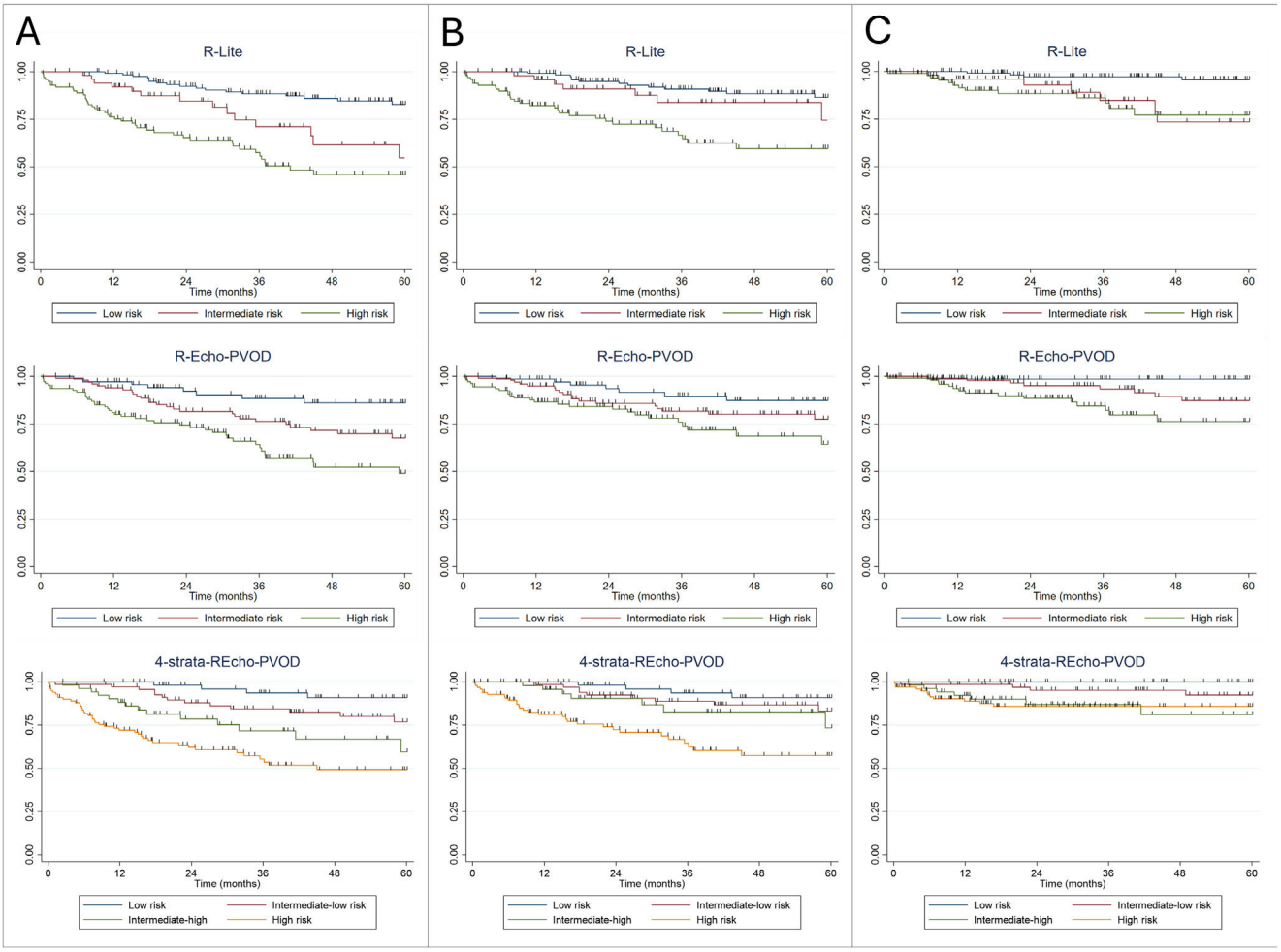

Fig. 2. Five-year Kaplan–Meier survival curves according to R-Lite, R-Echo-PVOD, and 4-strata-R-Echo PVOD models for (A) the composite endpoint (death or lung transplantation), (B) all-cause mortality, and (C) lung transplantation. REcho-PVOD: PVOD-adjusted REVEAL-Echo score; R-Lite: Reveal Lite 2.0; 4-strata R Echo-PVOD: combined four-strata model integrating R-Lite and R-Echo-PVOD.

Table 3
Reclassification of patients according to Reveal LITE 2.0 and PVOD-modified REVEAL ECHO.

		R-Echo-PVOD		
		Low	**Intermediate**	**High**
R-Lite	**Low**	Low 59 (20.9)	Low 54 (19.1)	Int-low 15 (5.3)
	Intermediate	Int-Low 8 (2.8)	Int-Low 17 (6.0)	Int-High 28 (9.9)
	High	High 5 (1.8)	High 29 (10.3)	High 67 (23.8)

Color legend: green = low risk; yellow = intermediate-low risk; orange = intermediate-high risk; red = high risk, according to the 4-strata risk classification system. Data are presented as *n* (%).

Table 4
Performance metrics of the predictive models evaluated for 1 and 5 years follow-up: REVEAL Lite 2.0, REVEAL-ECHO, PVOD-modified REVEAL-ECHO, and the combined Reveal Lite 2.0 + PVOD-modified REVEAL-ECHO model.

	R-Lite	R-Echo	R-Echo-PVOD	4-strata-R-Echo-PVOD
1-Year follow-up				
Harrell's *C* (CI 95%)	0.787 (0.734–0.840)	0.646 (0.553–0.739)	0.694 (0.612–0.777)	0.791 (0.742–0.839)
Somers' *D*	0.574	0.291	0.389	0.582
AUC (CI 95%)	0.789 (0.729–0.849)	0.642 (0.544–0.739)	0.696 (0.610–0.783)	0.794 (0.738–0.849)
AIC	279.4	307.5	299.8	278.2
5-Years follow-up				
Harrell's *C* (CI 95%)	0.703 (0.652–0.754)	0.583 (0.520–0.647)	0.651 (0.595–0.708)	0.716 (0.668–0.764)
Somers' *D*	0.408	0.167	0.299	0.431
AUC (CI 95%)	0.680 (0.614–0.746)	0.568 (0.495–0.640)	0.637 (0.572–0.702)	0.696 (0.633–0.759)
AIC	779.9	771.5	799.1	741.2

AIC: Akaike's Information Criterion; AUC: Area Under the Receiver Operating Characteristic Curve; Harrell's *C*: Harrell's concordance statistic; Somers' *D*: Somers' *D* rank correlation coefficient.

function—despite similar hemodynamics compared with non-PVOD patients. This suggests that the poor prognosis in PVOD may not be driven solely by hypoxemia or vasodilator intolerance, but also by more advanced baseline RV dysfunction. In this context, echocardiography provides incremental value over clinical markers (WHO functional class or six-minute walk distance), which may be confounded by respiratory impairment, thereby improving identification of patients likely to require earlier listing for LT.

These observations align with previous evidence suggesting that hypoxemia can directly affect RV structure and function, independently of afterload. In healthy individuals, hypoxia has been associated with increased RV dimensions, impaired RV relaxation, and a higher Tei index despite only modest elevations in RV systolic pressure [22,23]. Similarly, at the molecular level, disruption of HIF-1α in cardiomyocytes worsens RV remodeling during chronic hypoxia without increasing RV systolic pressure [24]. Clinically, hypoxemia-triggered myocardial infarction with non-obstructive coronary arteries has been reported in heritable PVOD, illustrating extreme oxygen supply–demand mismatch [25]. These findings support the hypothesis that adverse RV remodeling in PVOD may reflect the combined impact of PH, chronic hypoxemia and intrinsic myocardial maladaptation.

Risk stratification analysis in our cohort demonstrated that clinical models such as R-Lite performed robustly, even in a population with a high prevalence of PVOD. These findings are consistent with previous reports, where R-Lite achieved a C-index of 0.61 for mortality prediction in a PVOD cohort [16]. Notably, our study extends prior knowledge by demonstrating that R-Lite remains effective for the composite endpoint of death or LT, although it does not fully separate intermediate- from high-risk groups for LT alone at long-term follow-up.

Although R-Lite performed well in our cohort, integrating the echocardiographic model with PVOD etiology provided additional prognostic value. R-Echo-PVOD improved event reclassification compared with R-Lite by shifting a greater proportion of patients with adverse outcomes into higher-risk categories. This effect was especially evident in transplant-oriented analyses, supporting the clinical value of incorporating echocardiographic and disease-specific information into risk assessment. In addition, the 4-strata R-Echo-PVOD model further improved both event reclassification and overall reclassification performance, while providing the best discrimination for the composite endpoint. Among transplanted patients, the mean time from baseline assessment to waitlist inclusion decreased across increasing risk categories in both models; however, the low-risk group defined by R-Echo-PVOD showed the longest time to listing (46.2 months), exceeding that observed with R-Lite (36.0 months). This finding suggests that the echocardiographic component may improve identification of patients with a more stable clinical course.

Most importantly, concordant low-risk classification by both models yielded the highest negative predictive value, reaching 93.2% for death, 93.2% for the composite endpoint, and 100% for LT alone. Clinically, this combined low-risk profile may help identify patients who could be referred early to a transplant center for specialized follow-up without immediate waitlist inclusion, provided that close and repeated reassessment is maintained. Overall, these findings support a complementary approach to risk stratification, in which clinical and imaging information are integrated to improve prognostic assessment and guide decision-making more accurately than either domain alone.

Limitations

This was an observational single-center study based on retrospectively collected data. PH was defined using the hemodynamic

thresholds in place at the time of registry entry. Approximately 60% of patients lacked definitive histological or genetic confirmation of PVOD. However, diagnosis was adjudicated using previously published international criteria. To reduce misclassification, patients with relevant respiratory comorbidities were excluded. The lack of external validation poses a risk of limited generalizability. However, bootstrap resampling showed minimal optimism. This internal validation does not substitute the need for external validation in independent cohorts.

Conclusions

In this tertiary-center PAH cohort enriched for PVOD, this etiology was associated with disproportionate adverse RV remodeling despite similar baseline hemodynamics, and with higher rates of death and LT, including urgent LT. Incorporating PVOD as a weighted variable enhanced the performance of the echocardiography-based R-Echo framework, and the resulting 4-strata R-Echo-PVOD model showed the best overall prognostic performance, with better discrimination and reclassification across all endpoints. Concordant low-risk classification by both clinical and echocardiographic models was also associated with a high negative predictive value for adverse events, particularly transplant. These findings support the complementary use of clinical and echocardiographic risk assessment to refine prognostic stratification and improve transplant-related decision-making in populations with a high prevalence of PVOD.

Author contributions

EGO contributed to data collection, data analysis and interpretation, and drafting of the manuscript. CDS contributed to data collection. CJL-G, AC-U, PE-S and JPE contributed to conception and design. JPE performed a complete statistical review and revised the manuscript. SAC, MV, BB, IMDM, CAQL and FAY critically revised the manuscript. All authors approved the final version of the manuscript.

Artificial intelligence involvement

The authors declare that no artificial intelligence tools were used in the generation of the manuscript.

Funding

Alejandro Cruz-Utrilla holds a research contract Juan Rodes from the Instituto de Salud Carlos III, Ministerio de Ciencia, Innovación y Universidades, Spanish Government (JR23/00071) and a research grant I+D+I from the Instituto de Salud Carlos III, Ministerio de Ciencia, Innovación y Universidades, Spanish Government (PI24/01880). Eva Gutierrez Ortiz is supported by a Río Hortega Grant from the Instituto de Salud Carlos III (ISCIII, CM25/00215). Pilar Escribano-Subias holds a research grant I+D+I from the Instituto de Salud Carlos III, Ministerio de Ciencia, Innovación y Universidades, Spanish Government (PI21/01690).

Conflicts of interest

EGO reports honoraria from Janssen Pharmaceutica (Johnson & Johnson), MSD and Ferrer, and advisory board participation for Janssen. CJLG reports consulting fees from BeOne, honoraria from AOP Orphan, Ferrer, AstraZeneca, BeOne and Janssen (Johnson & Johnson), and advisory board participation for Pulmovant. ACU reports honoraria from AOP Orphan, Ferrer, Gossamer Bio, MSD and Janssen (Johnson & Johnson), and advisory board participation for Gossamer Bio, MSD and Janssen. PES reports honoraria from MSD, Ferrer, AOP Health, Gossamer and Janssen, and advisory board participation for MSD, Ferrer, Gossamer, AOP Health and Janssen. IMDM reports honoraria and advisory board participation from Janssen. MV reports honoraria from MSD, Janssen, Boston Scientific and SMT. BB reports honoraria from MSD and Janssen (Johnson & Johnson). JPE, SAC, CDS, CAQL and FAY declare no conflicts of interest.

Appendix A. Supplementary data

Supplementary data associated with this article can be found, in the online version, at doi:10.1016/j.arbres.2026.05.002.

References

[1] Humbert M, Kovacs G, Hoeper MM, Badagliacca R, Berger RMF, Brida M, et al. 2022 ESC/ERS Guidelines for the diagnosis and treatment of pulmonary hypertension. Eur Heart J 2022;43(38):3618–731, http://dx.doi.org/10.1093/eurheartj/ehac237.
[2] Chang KY, Duval S, Badesch DB, Bull TM, Chakinala MM, De Marco T, et al. Mortality in pulmonary arterial hypertension in the modern era: early insights from the pulmonary hypertension association registry. J Am Heart Assoc 2022;11(9):e024969, http://dx.doi.org/10.1161/JAHA.121.024969.
[3] El-Kersh K, Zhao C, Elliott G, Farber HW, Gomberg-Maitland M, Selej M, et al. Derivation of a risk score (REVEAL-ECHO) based on echocardiographic parameters of patients with pulmonary arterial hypertension. Chest 2023;163(5):1232–44, http://dx.doi.org/10.1016/j.chest.2022.12.045.
[4] Badagliacca R, Ghio S, D'Alto M, Ameri P, Correale M, Filomena D, et al. Relevance of echocardiography-derived phenotyping in patients with pulmonary arterial hypertension treated with initial oral combination therapy: an Italian Pulmonary Hypertension Network (iPHNET) study. Am J Respir Crit Care Med 2024;210(3):362–5, http://dx.doi.org/10.1164/rccm.202402-0431LE.
[5] Badagliacca R, Poscia R, Pezzuto B, Papa S, Reali M, Pesce M, et al. Prognostic relevance of right heart reverse remodeling in idiopathic pulmonary arterial hypertension. J Heart Lung Transplant 2017, http://dx.doi.org/10.1016/j.healun.2017.09.026. Published online October 2, S1053-2498(17)32041-7.
[6] Ghio S, Badagliacca R, D'Alto M, Scelsi L, Argiento P, Brunetti ND, et al. Right ventricular phenotyping in incident patients with idiopathic pulmonary arterial hypertension. J Heart Lung Transplant 2024;43(10):1668–76, http://dx.doi.org/10.1016/j.healun.2024.06.003.
[7] Montani D, Lau EM, Dorfmüller P, Girerd B, Jaïs X, Savale L, et al. Pulmonary veno-occlusive disease. Eur Respir J 2016;47(5):1518–34, http://dx.doi.org/10.1183/13993003.00026-2016.
[8] Navas P, Rodriguez Reguero JJ, Escribano Subías P, Founder mutation C. 3344C>t(p.Pro1115Leu) in the EIF2KA4 gene in iberian romani patients with pulmonary veno-occlusive disease: a warning for our daily practice. Arch Bronconeumol 2016;52(8):444–5, http://dx.doi.org/10.1016/j.arbres.2016.01.005.
[9] Navas Tejedor P, Palomino Doza J, Tenorio Castaño JA, Enguita Valls AB, Rodríguez Reguero JJ, Martínez Meñaca A, et al. Variable expressivity of a founder mutation in the EIF2AK4 gene in hereditary pulmonary veno-occlusive disease and its impact on survival. Rev Esp Cardiol (Engl Ed) 2018;71(2):86–94, http://dx.doi.org/10.1016/j.rec.2017.03.034.
[10] Tenorio J, Navas P, Barrios E, Fernández L, Nevado J, Quezada CA, et al. A founder EIF2AK4 mutation causes an aggressive form of pulmonary arterial hypertension in Iberian Gypsies. Clin Genet 2015;88(6):579–83, http://dx.doi.org/10.1111/cge.12549.
[11] Escribano-Subias P, Blanco I, López-Meseguer M, Jiménez López-Guarch C, Román A, Morales P, et al. Survival in pulmonary hypertension in Spain: insights from the Spanish registry. Eur Respir J 2012;40(3):596–603, http://dx.doi.org/10.1183/09031936.00101211.
[12] Badesch DB, Raskob GE, Elliott CG, Krichman AM, Farber HW, Frost AE, et al. Pulmonary arterial hypertension: baseline characteristics from the REVEAL Registry. Chest 2010;137(2):376–87, http://dx.doi.org/10.1378/chest.09-1140.
[13] Swinnen K, Quarck R, Godinas L, Belge C, Delcroix M. Learning from registries in pulmonary arterial hypertension: pitfalls and recommendations. Eur Respir Rev 2019;28(154):190050, http://dx.doi.org/10.1183/16000617.0050-2019.
[14] Organización Nacional de Trasplantes. Actividad de Donación y Trasplante Pulmonar España 2024; 2024. https://www.ont.es/wp-content/uploads/2025/03/ACTIVIDAD-DE-DONACION-Y-TRASPLANTE-PULMONAR-ESPANA-2024.pdf
[15] Cruz-Utrilla A, Pérez-Olivares C, Luna-López R, Jiménez López-Guarch C, Bedate P, Martínez Meñaca A, et al. Risk stratification in pulmonary veno-occlusive disease. Arch Bronconeumol 2024;60(5):321–3, http://dx.doi.org/10.1016/j.arbres.2024.02.011.
[16] Boucly A, Solinas S, Beurnier A, Jaïs X, Keddache S, Eyries M, et al. Outcomes and risk assessment in pulmonary veno-occlusive disease. ERJ Open Res 2024;10(1), http://dx.doi.org/10.1183/23120541.00612-2023, 00612-02023.
[17] Montani D, Girerd B, Jaïs X, Levy M, Amar D, Savale L, et al. Clinical phenotypes and outcomes of heritable and sporadic pulmonary veno-occlusive

disease: a population-based study. Lancet Respir Med 2017;5(2):125–34, http://dx.doi.org/10.1016/S2213-2600(16)30438-6.
[18] Galiè N, Humbert M, Vachiery JL, Gibbs S, Lang I, Torbicki A, et al. 2015 ESC/ERS Guidelines for the diagnosis and treatment of pulmonary hypertension: The Joint Task Force for the Diagnosis and Treatment of Pulmonary Hypertension of the European Society of Cardiology (ESC) and the European Respiratory Society (ERS): Endorsed by: Association for European Paediatric and Congenital Cardiology (AEPC), International Society for Heart and Lung Transplantation (ISHLT). Eur Heart J 2016;37(1):67–119, http://dx.doi.org/10.1093/eurheartj/ehv317.
[19] Pérez Núñez M, Alonso Charterina S, Pérez-Olivares C, Revilla Ostolaza Y, Morales Ruíz R, Enguita Valls AB, et al. Radiological findings in multidetector computed tomography (MDCT) of hereditary and sporadic pulmonary veno-occlusive disease: certainties and uncertainties. Diagnostics (Basel) 2021;11(1):141, http://dx.doi.org/10.3390/diagnostics11010141.
[20] Benza RL, Kanwar MK, Raina A, Scott JV, Zhao CL, Selej M, et al. Development and validation of an abridged version of the REVEAL 2.0 risk score calculator, REVEAL Lite 2, for use in patients with pulmonary arterial hypertension. Chest 2021;159(1):337–46, http://dx.doi.org/10.1016/j.chest.2020.08.2069.
[21] Collins GS, Reitsma JB, Altman DG, Moons KGM. Transparent reporting of a multivariable prediction model for individual prognosis or diagnosis (TRIPOD): the TRIPOD statement. BMJ 2015;350:g7594, http://dx.doi.org/10.1136/bmj.g7594.
[22] Netzer NC, Strohl KP, Högel J, Gatterer H, Schilz R. Right ventricle dimensions and function in response to acute hypoxia in healthy human subjects. Acta Physiol (Oxf) 2017;219:478–85, http://dx.doi.org/10.1111/apha.12740.
[23] Naeije R, Dedobbeleer C. Pulmonary hypertension and the right ventricle in hypoxia. Exp Physiol 2013;98(8):1247–56, http://dx.doi.org/10.1113/expphysiol.2012.069112.
[24] Nozik-Grayck E, Shimoda LA. Heart of the matter: divergent roles of hypoxia-inducible factors in hypoxia-induced right ventricle hypertrophy. Am J Respir Cell Mol Biol 2020;63(5):549–50, http://dx.doi.org/10.1165/rcmb.2020-0325ED.
[25] Ortiz-Bautista C, Bueno H, Escribano-Subías P. Myocardial injury in severe heritable pulmonary veno-occlusive disease. J Heart Lung Transplant 2017;36(7):818–20, http://dx.doi.org/10.1016/j.healun.2017.02.013.